16B.1 A FRESH LOOK AT THE RANGE WEIGHTING FUNCTION FOR MODERN WEATHER RADARS

Sebastián Torres and Christopher Curtis

Cooperative Institute for Mesoscale Meteorological Studies, The University of Oklahoma and
NOAA/OAR National Severe Storms Laboratory
Norman, Oklahoma

1. INTRODUCTION

The range weighting function (RWF) is normally introduced in discussions of the radar resolution volume because it defines the radial extent of such volumes. The RWF determines how individual scatterer contributions are weighted as a function of range to produce estimates of the meteorological variables associated with a single resolution volume. The RWF is commonly defined in terms of the transmitter pulse envelope and the receiver filter impulse response and determines the range resolution of a radar. Digital signal processing of echo samples along the range-time dimension (herein referred to as range-time processing) can also modify the effective RWF. This third contributor to the RWF has become more significant as novel range-time processing techniques (e.g., those that operate on range oversampled signals) have become feasible for real-time implementation on modern radar systems. The impact of range-time processing on the RWF is the focus of this paper. The effects of different types of range-time processing on the RWF are examined using typical processing schemes.

The relationship between the RWF and range resolution has already been mentioned, but the RWF is important for several other reasons. Reflectivity gradients can cause biases in reflectivity estimates and can also shift the range location assigned to these data (Mueller 1977; Johnston et al. 2002). Additionally, the combination of the RWF and the resolution volume spacing determines the correlation between meteorological data in range. This range correlation affects the variance reduction when meteorological-variable estimates are averaged along range to gain data precision at the cost of reduced range resolution. Finally, the RWF can also affect the performance of algorithms that process meteorological data. For example, changes in the effective resolution volume in angular and/or range extents can affect tornado detection algorithms that utilize Doppler velocity signatures (Wood and Brown 1997; Torres and Curtis 2006). These effects can be further complicated by the fact that some range-time processing techniques produce a different RWF at each resolution volume. An example is adaptive pseudowhitening; it uses a different linear transformation based on measurements of signal characteristics (e.g., signal-to-noise ratio and spectrum width) at every resolution volume (Curtis and Torres 2011). Because of these significant effects, it is important to understand how range-time processing affects the RWF.

In this paper, we compute the RWF arising from the processing of echo samples along the range-time dimension. It uses two elements: (1) a pulse matrix which is based on the transmitter pulse envelope and the receiver filter and (2) a transformation matrix which is determined by the type of range-time processing, thus capturing all three major contributors to the RWF: transmitter pulse envelope, receiver filter, and range-time processing.

2. THE RANGE WEIGHTING FUNCTION

In this section we derive a general formulation of the RWF that includes the effects of range-time signal processing.

2.1. Model Description

Assume that the scatterers illuminated by the transmitted pulse (as it propagates in the radial direction away from the radar) can be modeled as a linear array of independent "scattering centers" uniformly spaced in range. The spacing between adjacent scattering centers is large compared to the radar wavelength but small compared to the range extent of the transmitter pulse. In this model, each scattering center represents the combined echo contributions (weighted by the two-way antenna beam pattern in azimuth and elevation) from all scatterers in an elemental spherical shell of thickness $\Delta r = c\Delta\tau_s / 2$, where c is the speed of light and $\Delta\tau_s$ is much smaller than the transmitter pulse width, τ. As with most modern radar receivers, we assume that sampling at the rate T_r^{-1} occurs after all receiver filters and down-conversion to baseband but before any range-time signal processing. This sampling at the receiver produces discrete-time in-phase and quadrature (range oversampled *I* and *Q*) signals, herein referred to as time-series data.

i. Transmission and Reception Models

The *n*-th scattering center would produce a baseband analog voltage δV_r at the receiver's front end of the same form as the envelope of the transmitter pulse. The baseband voltage δV_o after all receiver filters but before the receiver sampling can be obtained by convolving the input waveform with the baseband-equivalent impulse response of the receiver filter. Assume that the receiver sampling period is $T_r = F\Delta\tau_s$,

Corresponding *author address:* Sebastián M. Torres, NSSL, 120 David L. Boren Blvd., Norman, OK 73072; email: Sebastian.Torres@noaa.gov

where F is an integer. This creates (range-oversampled) time-series data with corresponding resolution volumes spaced at $\Delta R = cT_r/2 = F\Delta r$. Finally, summing the contributions of all scattering centers, S, at range time IT_r, the time-series data V (i.e., the sampled received complex voltage) can be expressed as

$$V(IT_r, mT_s) = \sum_n S(n\Delta r, mT_s)p[(IF - n)\Delta\tau_s], \qquad (1)$$

where the "modified pulse" p is the envelope of the transmitted pulse smoothed by the receiver filter; thus, p includes the first two contributors to the RWF as described in the introduction. In a well-designed radar, p must decay quickly away from its peak in order to achieve acceptable range localization of echoes. Hence, assume that $p(n\Delta\tau_s)$ is (or can be approximated to be) non-zero only for $0 \le n < N_p$, where $N_p\Delta\tau_S$ is the modified-pulse length in seconds. Thus, for $IF > N_p$, the convolution in (1) becomes

$$V(I,m) = \sum_{n=IF-N_p+1}^{IF} S(n,m)p(IF - n), \qquad (2)$$

where the range- and sample-time sampling periods were dropped to simplify the notation.

Next, assume that N_v-by-M samples are needed to produce a set of meteorological variables for an arbitrary resolution volume and that these samples are indexed by $I_0 \le I < I_0 + N_v$ along range time and by $0 \le m < M$ along sample time, where I_0T_r is an arbitrary range time. The time-series data needed to produce a set of meteorological variables can be obtained from (2) and written in matrix form as

$$\mathbf{V}_m = \mathbf{P}\mathbf{S}_m, \qquad (3)$$

where $\mathbf{V}_m = \left[V(I_0,m),\cdots,V(I_0+N_v-1,m)\right]^T$ is the vector of N_v (range-oversampled) time-series data at sample time m, $\mathbf{S}_m = \left\{S[I_0F - N_p + 1, m],\cdots,S[I_0F + (N_v-1)F, m]\right\}^T$ is the vector of $N_s = N_p + (N_v - 1)F$ scattering center voltages at sample time m, and $\mathbf{P}$ is the N_v-by-N_s modified-pulse convolution matrix (herein referred to as the pulse matrix). The pulse matrix can be written as

$$\mathbf{P} = \begin{bmatrix} \tilde{\mathbf{p}}_0 \\ \tilde{\mathbf{p}}_F \\ \vdots \\ \tilde{\mathbf{p}}_{(N_v-1)F} \end{bmatrix}, \qquad (4)$$

where $\tilde{\mathbf{p}}_0 = \left[p(N_p - 1),\cdots,p(1),p(0),0,\cdots,0\right]$, is the time-reversed modified-pulse vector zero-padded to N_S elements, and $\tilde{\mathbf{p}}_n$ is $\tilde{\mathbf{p}}_0$ circularly shifted to the right by n elements. That is, each row of $\mathbf{P}$ is formed by circularly shifting the previous row F times to the right. This pulse matrix captures the effects of the first two contributors to the RFW: the transmitted pulse envelope and the receiver filter.

ii. Range-Time Signal Processing Model

Range-oversampled time-series data are processed to obtain autocovariance estimates for one resolution volume. The signal processing that occurs along the range-time dimension is, as mentioned previously, the third contributor to the RWF. A generalized model for the range-time processing involves two steps: transformation and estimation. Transformed signals at sample-time m, $\mathbf{X}_m$, are obtained as

$$\mathbf{X}_m = \mathbf{T}\mathbf{V}_m, \qquad (5)$$

where $\mathbf{T}$ is a complex-valued N_x-by-N_v transformation matrix. This transformation produces N_x samples, where N_x does not need to be equal to N_v. From these transformed samples, the lag-k autocovariance can be estimated as

$$\hat{R}(k) = \frac{1}{N_x(M - |k|)} \sum_{m=0}^{M-|k|-1} \mathbf{X}_m^H \mathbf{D} \mathbf{X}_{m+k}, \qquad (6)$$

where $\mathbf{D}$ is a complex-valued N_x-by-N_x autocovariance range-weighting matrix, and superscript H denotes conjugate transpose. A few typical processing cases are presented next to illustrate the applicability of this general range-time signal processing model.

CASE A: DIGITAL MATCHED FILTERING WITHOUT RANGE AVERAGING

This is the type of processing common to many weather radar systems with digital receivers, such as the Weather Surveillance Radar-1988 Doppler (WSR-88D), and can be represented with the two-step model as

$$\mathbf{X}_m = \mathbf{h}_{MF}\mathbf{V}_m, \qquad (7)$$

and

$$\hat{R}(k) = \frac{1}{M - |k|} \sum_{m=0}^{M-|k|-1} \mathbf{X}_m^H \mathbf{X}_{m+k}. \qquad (8)$$

Typically, k values (lags) of 0 and 1 are sufficient for the computation of reflectivity, Doppler velocity, and spectrum width estimates for a resolution volume. Here, $\mathbf{h}_{MF}$ is the 1-by-L eigenvector corresponding to the maximum eigenvalue of the normalized range-correlation matrix $\mathbf{C}_V$, where L is the range oversampling factor. $\mathbf{C}_V$ can be computed as $\mathbf{C}_V = \|\mathbf{p}\|^{-2}\mathbf{P}^*\mathbf{P}^T$, where $\|.\|$ is the vector-norm operator. It is easy to see that for this case $N_V = L$, $N_x = 1$, $\mathbf{D} = 1$, and $\mathbf{T} = \mathbf{h}_{MF}$.

CASE B: WHITENING (OR PSEUDOWHITENING) WITHOUT RANGE AVERAGING

Range oversampling and whitening (or pseudowhitening) is a technique that can be used to improve the precision of spectral moment and polarimetric variable estimates on weather radars. Range oversampling provides more samples for the estimation of meteorological variables; these samples can be transformed (decorrelated) and efficiently used to reduce the variance of estimates and/or reduce the required observation (dwell) times (Torres and Zrnić

2003). This type of processing has been implemented on the National Weather Radar Testbed (NWRT) phased-array radar (PAR) and is its default mode of operation (Curtis and Torres 2011). Range oversampling and whitening (or pseudowhitening) can be modeled as follows:

$$\mathbf{X}_m = \mathbf{W}\mathbf{V}_m \,, \tag{9}$$

and

$$\hat{R}(k) = \frac{1}{L(M-|k|)} \sum_{m=0}^{M-|k|-1} \mathbf{X}_m^H \mathbf{X}_{m+k} \,, \tag{10}$$

where L is the range oversampling factor. For this case, $N_x = N_v = L$, $\mathbf{D} = \mathbf{I}$ (the L-by-L identity matrix), and $\mathbf{T} = \mathbf{W}$ (a range-oversampling transformation matrix). $\mathbf{W}$ can be either the L-by-L whitening matrix obtained as the inverse square root of $\mathbf{C}_V$ (i.e., $\mathbf{W} = \mathbf{H}^{-1}$, where $\mathbf{C}_V = \mathbf{H}^*\mathbf{H}^T$) or a more general L-by-L pseudowhitening matrix as described by Torres et al. (2004).

CASE C: DIGITAL MATCHED FILTERING WITH RANGE AVERAGING

This is the type of range-time processing that entails averaging consecutive estimates along range for greater data precision at the expense of coarser range resolution. For example, the 1-km legacy-resolution reflectivity data produced by the WSR-88D is computed from the average of four signal-power estimates spaced 250-m apart. This type of processing can be represented with the two-step model as

$$\mathbf{X}_m = \begin{bmatrix} \mathbf{h}_{MF} & \mathbf{0}_L & \cdots & \mathbf{0}_L \\ \mathbf{0}_L & \mathbf{h}_{MF} & \cdots & \mathbf{0}_L \\ \vdots & \vdots & \ddots & \vdots \\ \mathbf{0}_L & \mathbf{0}_L & \cdots & \mathbf{h}_{MF} \end{bmatrix} \mathbf{V}_m \,, \tag{11}$$

and

$$\hat{R}(k) = \frac{1}{R(M-|k|)} \sum_{m=0}^{M-|k|-1} \mathbf{X}_m^H \mathbf{X}_{m+k} \,, \tag{12}$$

where R is the number of estimates in range to average (R = 4 for the WSR-88D legacy-resolution reflectivity), and $\mathbf{0}_L$ denotes a row vector of L zeros. For this case, $N_v = RL$, $N_x = R$, $\mathbf{D}$ is the R-by-R identity matrix, and $\mathbf{T}$ is the R-by-RL transformation matrix with shifted matched-filter entries as shown explicitly in (11).

CASE D: DIGITAL MATCHED FILTERING WITH RANGE INTERPOLATION

This type of processing can be useful when there is a point target (e.g., an aircraft) in an isolated resolution volume that obscures the meteorological data in the same volume. By assuming spatial uniformity of meteorological fields, data can be "rebuilt" using range interpolation of non-contaminated estimates. For example, the WSR-88D runs a strong-point clutter filter that detects and flags isolated resolution volumes with significant contamination by looking for abrupt discontinuities in a range profile of received signal powers. Autocovariances corresponding to flagged resolution volumes are obtained through linear interpolation (averaging) of neighboring non-contaminated values (Unisys Corporation 1991). This type of processing can be represented with the two-step model as

$$\mathbf{X}_m = \begin{bmatrix} \mathbf{h}_{MF} & \mathbf{0}_L & \mathbf{0}_L \\ \mathbf{0}_L & \mathbf{h}_{MF} & \mathbf{0}_L \\ \mathbf{0}_L & \mathbf{0}_L & \mathbf{h}_{MF} \end{bmatrix} \mathbf{V}_m \,, \tag{13}$$

and

$$\hat{R}(k) = \frac{1}{3(M-|k|)} \sum_{m=0}^{M-|k|-1} \mathbf{X}_m^H \begin{bmatrix} 3/2 & 0 & 0 \\ 0 & 0 & 0 \\ 0 & 0 & 3/2 \end{bmatrix} \mathbf{X}_{m+k} \,. \tag{14}$$

This case is similar to the previous one except that R = 3 and $\mathbf{D}$ is a nontrivial matrix. Here, $N_v = 3L$, N_x = 3, $\mathbf{D}$ is the 3-by-3 matrix in (14), and $\mathbf{T}$ is the 3-by-3L transformation matrix with shifted matched-filter entries in (13).

These cases cover many common types of range-time processing and illustrate the generality of the proposed signal processing model. Other more complex approaches such as overlapped averaging in range, range filtering, and the efficient implementation of adaptive pseudowhitening (Curtis and Torres 2011) can also be represented with this model.

2.2. Range Weighting Function Computation

To compute the RWF using the proposed model, start by taking the expected value of (6). That is,

$$E\left[\hat{R}(k)\right] = \frac{1}{N_x(M-|k|)} \sum_{m=0}^{M-|k|-1} E\left[\mathbf{X}_m^H \mathbf{D} \mathbf{X}_{m+k}\right]. \tag{15}$$

After some manipulation, this can be written as

$$E\left[\hat{R}(k)\right] = \frac{1}{N_x} \sum_{n=1}^{N_s} \{\mathbf{Q}\}_{nn} R^{(S)}_{S(I_0F-N_p+n)}(k) \,, \tag{16}$$

where $\mathbf{Q} = \mathbf{P}^H\mathbf{T}^H\mathbf{D}\mathbf{T}\mathbf{P}$ is an N_S-by-N_S matrix, superscript (S) denote sample-time autocovariance, and the scattering centers for the range-time autocovariance are explicitly identified because stationarity in range is not assumed. Eq. (16) shows that sample-time autocovariance estimates at an arbitrary resolution volume consist of *weighted* contributions of sample-time autocovariances from scattering centers $I_0F - N_p + 1$ to $I_0F - N_p + N_s$. These weights, the diagonal entries of $\mathbf{Q}/N_x$, are in fact the RWF, herein denoted by w and defined as

$$w(n\Delta r) = \begin{cases} N_x^{-1}\left\{\mathbf{P}^H\mathbf{T}^H\mathbf{D}\mathbf{T}\mathbf{P}\right\}_{nn} & I_0F - N_p < n \le I_0F + (N_v - 1)F \\ 0 & \textit{otherwise} \end{cases} . \tag{17}$$

Eq. (17) provides the functional form of the RWF but does not provide explicit range localization. In other words, the range to be assigned to meteorological variables computed from the set of N_v time-series data samples beginning at time I_0T_r is not obvious. However, the support of function w is the interval defined by $\Delta r(I_0F - N_p + 1)$ and $\Delta r[I_0F + (N_v - 1)F]$, so it seems logical that meteorological data be assigned to the

range location corresponding to the middle point of this interval; i.e.,

$$r_0 = \left[l_0 F + \frac{(N_v - 1)F - N_p + 1}{2} \right] \Delta r \ . \qquad (18)$$

Another common way to assign range location is by considering the maximum of w; however, this definition does not work well for all types of range-time processing such as those that produce multi-modal RWFs. Still, for any of these range assignments to be valid, all the scattering centers located in the support of the RWF must exhibit the same statistical properties in range (i.e., range stationarity). If this does not hold, as in the case of reflectivity gradients, the range assignment must be corrected as described by Mueller (1977) or Johnston et al. (2002).

Fig. 1 shows the normalized RWFs corresponding to the previously introduced cases with the specific signal-processing model parameters listed in Table 1. The RWFs are plotted as a function of range relative to their center or assigned range location r_0 (i.e., zero corresponds to r_0). Range values are plotted in $L\Delta R$ units because this is the typical spacing of meteorological-data resolution volumes. For all cases, F = 20 (i.e., $T_r = 20\Delta\tau_s$) and the range-oversampling factor is L = 4. The cases depicted in the top panel correspond to the idealized case of a rectangular transmitter pulse envelope and a noiseless receiver having a receiver filter with very large bandwidth, $B_6 \gg \tau^{-1}$ (recall that this is the bandwidth prior to any range-time processing such as digital matched filtering). The length of the idealized modified pulse is $4T_r$. The cases in the middle and bottom panels correspond to the modified pulse of the NWRT PAR, which is more realistic with a length of $6T_r$. Both modified pulses are shown in Fig. 2.

For cases *a* and *b* with an idealized modified pulse, the depicted RWFs vary from peaky to almost flat as the processing changes from matched filter to whitening by stepping through varying degrees of pseudowhitening using a "sharpening filter" with parameter α, where $0 \le \alpha \le 1$ (Torres et al. 2004). Not surprisingly, as the sharpening filter's performance (in terms of variance reduction) goes from matched filter ($\alpha \to 0$) to whitening (α = 1), its corresponding RWF becomes broader and variance reduction improves. For the NWRT PAR modified pulse, the RWFs exhibit a similar trend but they also become more asymmetric about r_0 due to the asymmetry and nontrivial phase of the modified pulse.

The RWFs corresponding to processing cases *c* and *d* are examples of multi-modal RWFs, which are based on the digital-matched-filter RWF (case *a*). As expected, for processing that involves averaging consecutive meteorological-variable estimates in range (case *c*), the RWF consists of R shifted "replicas" of the RWF prior to averaging. On the other hand, for processing that involves range interpolation of meteorological-variable estimates (case *d*), it is evident that one or more of the central scattering centers do not contribute at all to the meteorological data. In all these cases, r_0 corresponds to the middle of the RWF, as defined.

Although the shape of the RWF conveys important information, a more concise way to characterize and compare the RWFs for different types of processing is by looking at the corresponding range resolution. The RWF also determines the correlation of meteorological data in range. Both of these are addressed in the next section.

3. RANGE RESOLUTION AND RANGE CORRELATION

The range resolution is directly related to the size of the radar resolution volume. For point targets, the range resolution measures the ability of the radar to distinguish two targets along a given direction. For weather radars, distributed meteorological scatterers are the targets of interest, but the range resolution is still important for observing fine-scale phenomena such as tornado vortices.

As shown in the previous section, processing along the range-time dimension affects the RWF, and this has the potential to change the radar range resolution. The standard way to define the range resolution for weather radars is in terms of the resolution volume. Doviak and Zrnić (1993) define the resolution volume as the volume circumscribed by the 6-dB contour of the product of the two-way antenna beam pattern and the RWF. The range resolution, denoted by r_6, is defined as the 6-dB width of the RWF. In this case, the 6-dB decrease is measured from the ends of the RWF with respect to the maximum value. This approach removes ambiguity when computing the width of multimodal RWFs (e.g., case *c* in Fig. 1).

Fig. 3 shows the 6-dB (r_6) widths plotted for cases *a* and *b* (Fig. 1) using the idealized and NWRT PAR modified pulses (Fig. 2). For the idealized pulse, the width is approximately $0.76L\Delta R$ for the digital matched filter. These values are given in $L\Delta R$ units which correspond to the meteorological-data resolution-volume spacing. As expected, the range width increases (i.e., the range resolution becomes coarser) as the RWF becomes less peaky; the width increases to about $1.76L\Delta R$ for range oversampling with a whitening transformation. There are jumps in the range resolution for the idealized pulse because of the discontinuities in the RWF. For the more realistic NWRT PAR modified pulse, the widths are slightly reduced (except for the matched filter) due to the larger roll-off factor, but the same effect can be seen. The values range from $0.9L\Delta R$ for the digital matched filter to $1.58L\Delta R$ for whitening. In the idealized case, the range width increases by a factor of 2.3 when using whitening compared to digital matched filtering while it only increases by 1.75 for the NWRT PAR modified pulse. In both cases, the range width for whitening increases to a value greater than the resolution volume spacing which shows that there is more overlap in range than typically. The effect of this overlap will be quantified later by examining the range correlation.

For case *d* with the NWRT PAR modified pulse, the width is calculated from the ends so $r_6 \approx 2.9L\Delta R$. This is consistent with computing the meteorological variables

by interpolating non-obscured data from resolution volumes on either side of the contaminated resolution volume. For case *c*, $r_6 \approx 3.9L\Delta R$; that is, the width matches what we would expect from averaging four matched-filter samples.

In addition to computing the range resolution, the RWF can be used to calculate the correlation between meteorological data from two adjacent resolution volumes. The correlation coefficient is computed by summing the products of the RWF values that overlap and then scaling so that the value is one for completely overlapping RWFs (i.e., zero range spacing). The correlation coefficient between data from adjacent resolution volumes is shown in Fig. 4 for both the idealized modified pulse and the more realistic modified pulse measured on the NWRT PAR. As in Fig. 3, the data corresponds to cases *a* and *b*. The correlation coefficient in the idealized case ranges from about 0.07 for digital-matched-filtered processing to 0.47 for range oversampling and whitening. For the NWRT PAR modified pulse, the correlation coefficient is approximately 0.03 for matched-filtered processing and 0.32 for whitening. This clearly quantifies the expected increase in correlation between the two types of processing. Another way to use the correlation is to examine how far apart resolution volumes for data obtained with range oversampling and whitened would need to be to have the same correlation coefficient as adjacent resolution volumes with matched-filtered data. For the idealized case, the meteorological-data resolution-volume spacing would need to increase by a factor of about 1.65 to have the same correlation as digital-matched-filtered processing and by a factor of about 1.5 for the case using the NWRT PAR modified pulse.

In summary, the RWF is a tool that can be used to examine the effects of different types of range-time processing. In this section, we used it to study the effects of range-time processing on both the range resolution and range correlation.

4. CONCLUSIONS

We derived a new formulation of the range weighting function (RWF) for weather radars that includes the effects of range-time signal processing. Traditionally, the RWF has been defined solely in terms of the transmitter pulse envelope and the receiver filter impulse response. However, we showed that signal processing techniques that operate along the range-time dimension (e.g., range oversampling, range averaging, and range interpolation) can also modify the effective RWF. This contributor to the RWF has gained significance in recent years as advanced range-time processing techniques have become feasible for real-time implementation on modern radar systems.

This new formulation will be useful for characterizing modern radar systems that operate on range oversampled signals (either by employing a digital matched filter or by exploiting more advanced processing techniques) and to evaluate the impact that signal processing has on the performance of algorithms that rely on spatial features of meteorological data.

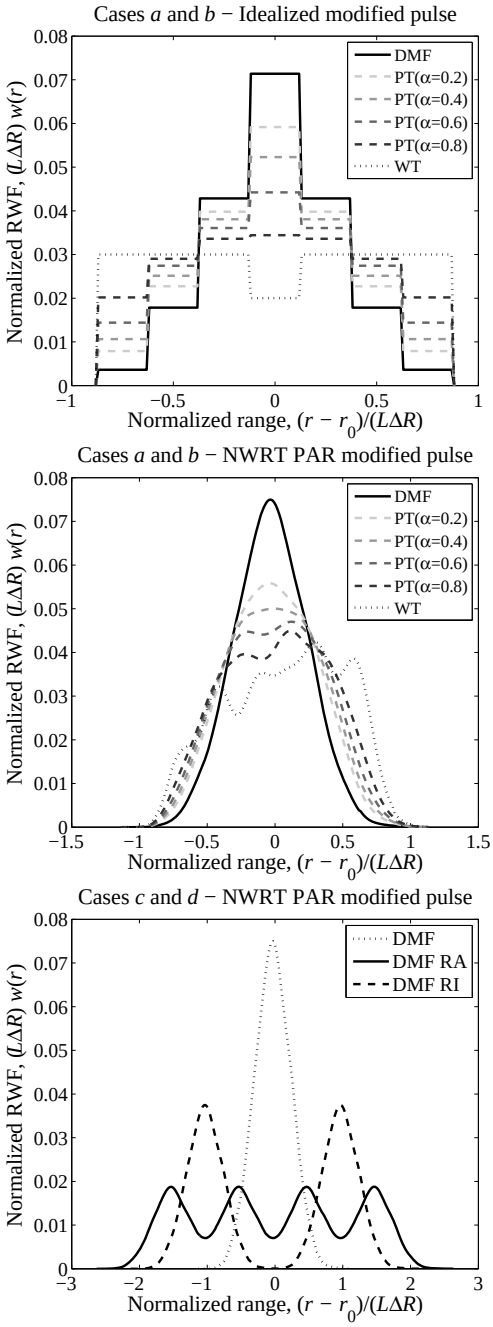

Fig. 1. Normalized RWFs corresponding to the cases in section 2.1 as a function of normalized range. The top and middle panels show the RWF for cases *a* and *b*; i.e., digital matched filtering (DMF), whitening transformation (WT), and pseudowhitening transformation (PT) based on a "sharpening filter" with parameter α = 0.2, 0.4, 0.6, and 0.8. The bottom panel shows the RWF for cases *c* and *d*; i.e., a digital matched filter with range averaging (DMF RA), and a digital matched filter with range interpolation (DMF RI); case *a* (DMF) is also included as a reference.

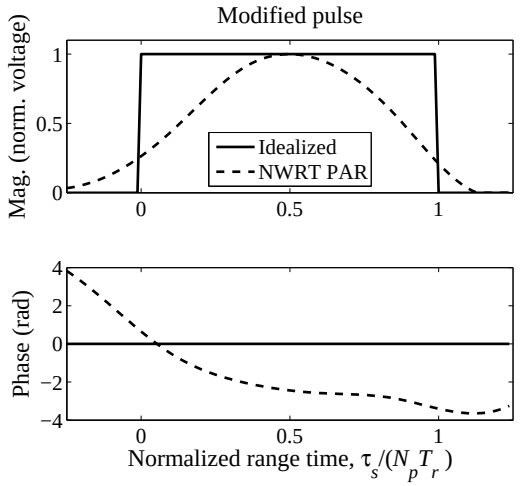

Fig. 2. Magnitude and phase of the idealized and NWRT PAR modified pulses.

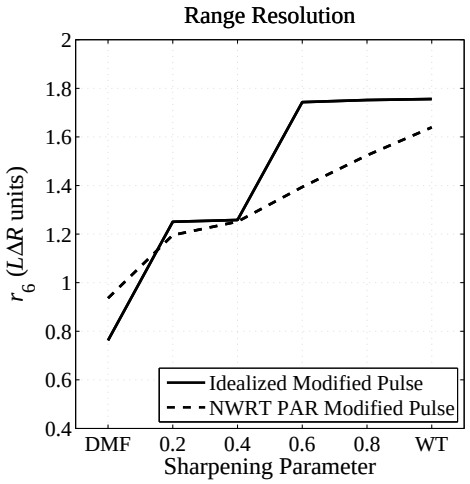

Fig. 3. Range resolution for cases *a* and *b* including a digital matched filter (DMF), a whitening transformation (WT), and pseudowhitening transformations with varying sharpening parameter α.

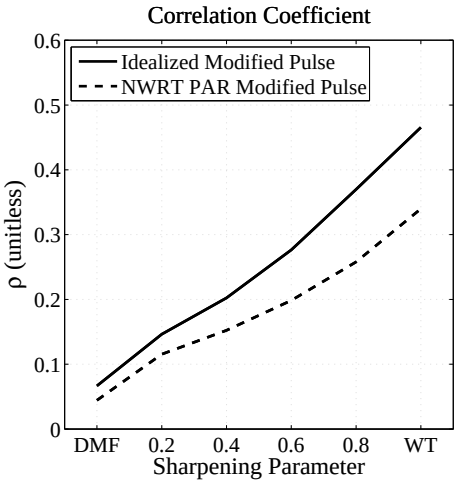

Fig. 4. Correlation coefficient between meteorological data from adjacent resolution volumes with range spacing of $L\Delta R$ for cases *a* and *b*.

ACKNOWLEDGMENT

This conference paper was prepared with funding provided by NOAA/Office of Oceanic and Atmospheric Research under NOAA-University of Oklahoma Cooperative Agreement #NA17RJ1227, U.S. Department of Commerce. The statements, findings, conclusions, and recommendations are those of the author(s) and do not necessarily reflect the views of NOAA or the U.S. Department of Commerce.

REFERENCES

Curtis, C. and Torres, S., 2011: Adaptive range oversampling to achieve faster scanning on the National Weather Radar Testbed Phased Array Radar. *J. Atmos. Oceanic Technol.*, in press.

Doviak, R.J., and D.S. Zrnić, 1993: *Doppler Radar and Weather Observations*. 2d ed. Academic Press, Inc., 562 pp.

Johnston, P. E., L. M. Hartten, C. H. Love, D. A. Carter, and K. S. Gage, 2002: Range Errors in Wind Profiling Caused by Strong Reflectivity Gradients. *J. Atmos. Oceanic Technol.*, **19**, 934–953.

Mueller, E. A., 1977: Statistics of High Radar Reflectivity Gradients. *J. Appl. Meteor.*, **16**, 511–513.

Torres, S., and D. Zrnić, 2003: Whitening in range to improve weather radar spectral moment estimates. Part I: Formulation and simulation. *J. Atmos. Oceanic Technol.*, **20**, 1433-1448.

Torres, S., and C. D. Curtis, 2006: Design considerations for improved tornado detection using super-resolution data on the NEXRAD network. *Preprints, 4th European Conf. on Radar Meteorology and Hydrology (ERAD)*, Barcelona, Spain, Copernicus.

Torres, S., C. Curtis, and J. R. Cruz, 2004: Pseudowhitening of weather radar signals to improve spectral moment and polarimetric variable estimates at low signal-to-noise. *IEEE Trans. Geosci. Remote Sensing*, **42**, 941-949.

Unisys Corporation, 1991: Computer program development specification for signal processing program (B5, CPCI 02), DV1208261F.

Wood, V. T., and R. A. Brown, 1997: Effects of Radar Sampling on Single-Doppler Velocity Signatures of Mesocyclones and Tornadoes. *Wea. Forecasting*, **12**, 928–938.